Tensile properties and damage evolution in C/SiC composite

Zheng He, Xuan Gu [*], Xiaoyu Sun, Jianxin Teng, YingShu Pang

College of Aerospace and Civil Engineering, Harbin Engineering University, Harbin 150001 China

[a] guxuan@hrbeu.edu.cn

Abstract

The tension–tension fatigue properties were investigated for a 2.5D-C/SiC composite in warp and weft direction. The fatigue experiments were carried out at room temperature (RT) and 900 °C in laboratory air. The tensile properties of the specimens survived 106 cycles were determined to explore the damage mechanisms. The fracture surfaces were examined by a scanning electron microscope. The composite exhibits excellent fatigue resistance at RT. The fatigue limits in both directions are about 85% of the ultimate tensile strength. The tensile strength and failure strain of the C/SiC can be enhanced for the survived composite at RT. The fatigue limits of the composite at 900 °C are much lower than those at RT in both directions. Examination of the fracture surfaces revealed that the failure is closely related to the propagation of the cracks originated from the crossover of the bundles and produced within the bundles. The cracks also offered the channels for the oxygen to penetrate into the composite and are responsible for the oxidization of the carbon fibers in the composite. The oxidization of the fibers plays a critical key role in decreasing the fatigue limits at 900 °C.

Keywords

Carbon fiber reinforced silicon carbide composites; Fatigue; Matrix cracking; Oxidation.

1. Introduction

Carbon fiber reinforced silicon carbide composites (C/SiCs) overcome the brittleness and low reliability of monolithic ceramics. Therefore, they are widely used as structural materials in different fields including advanced engines [1], gas turbines for power/steam co-generation [2], heat exchangers [3], as well as future nuclear reactors [4]. Components made of C/SiC are expected to experience loading fluctuations during operation in most potential applications, such as blades, disks, and piston rings in gas turbine. The cyclic loading can lead to damage accumulation and eventually to composite failure [5]. Furthermore, the degradation of the composites is further accelerated in the presence of moisture [6]. Hence, it is essential to clearly understand the fatigue behavior of C/SiC. Much experimental works were conducted to reveal the underlying damage mechanisms during fatigue. It is revealed that the main damage mechanisms involved the matrix cracking, interfacial sliding and degradation of the fiber strength [7]. Compared with one dimensional composite, additional matrix damage is observed in woven materials [8], particularly around the crossover points of the tow weaves. Matrix cracking intensifies at the crossover point [9], and result in debonding and delamination between the longitudinal and transverse tows due to strain mismatch [10]; [11]. Moreover, the fiber bundles may be split internally, often due to the coalescence of shear cracks emanating from adjacent transverse tows [12]; [13]. In order to overcome the shortages, a 2.5D-C/SiC was developed, whose reinforcement was composed of layers of straight weft yarns and a set of sinusoidal warp yarns. The interlaminar strength of 2.5D-C/SiC is improved significantly due to interlaced warp yarns in the adjacent layers [14]. In present work, the fatigue properties of the composites were investigated at room temperature (RT) and 900 °C. The fracture morphology was

studied by a scanning electron microscope (SEM). In addition, the residual tensile properties of the survived specimens were determined.

2. Experimental

The 2.5D-C/SiC composite was reinforced by a 2.5D woven perform, shown in Fig. 1. The reinforcement was made of T-300 carbon fibers. Each yarn contained 6000 fibers. The densities of the fiber in warp and weft direction are 10 and 3 ends/cm, respectively. A low-pressure chemical vapor infiltration (CVI) was used to prepare the composite. The PyC interphase with thickness of 0.2 μm was deposited with C3H6 at 1173 K and 5 kPa. Methyltrichlorosilane (MTS, CH3SiCl3) was used for the deposition of SiC matrix by CVI. After the deposition of SiC, the contoured, edge-loaded test specimens, shown in Fig. 2, were machined from the fabricated plates. Then, the specimens were further coated with a SiC coating of about 50 μm in thickness. The shape of the specimen was in agreement with ASTM: C1275. However, due to the limitation of the sheet, the length of the whole specimen was shortened. Other dimensions satisfied the requirement of ASTM. The fiber volume fraction and porosity are 40% and the 17%, respectively.

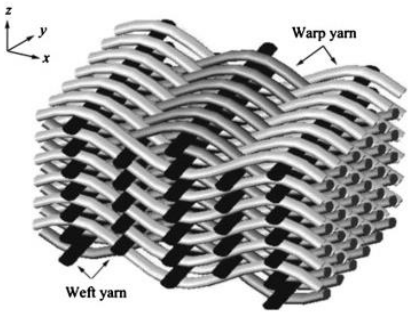

Fig. 1. Schematic of reinforcement in 2.5D-C/SiC.

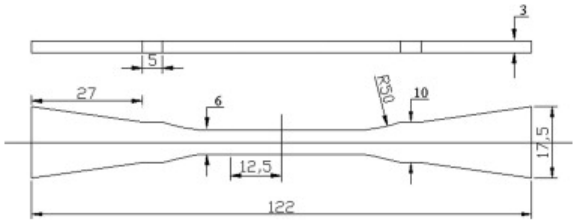

Fig. 2. Dimension of the specimen used for the tensile and fatigue experiments (in mm).

The fracture morphology of the failed specimens was examined by a SEM (HITACHI S-4700, Japan). In order to examine the damage in the composite, some samples were cut in the gauge section along the parallel the loading direction, and cold mounted and polished. The polished samples were also examined by SEM.

3. RESULTS AND DISCUSSION

Fig. 3 shows the representative tensile stress–strain curves for the 2.5D-C/SiC at 900 °C. Because of part of the curve coincide with the curve in warp direction, it is difficult in making a difference between both curves. A translation of the curve for the composite in weft direction was made by 0.1%. Both curves exhibit a linear response near the origin and a following nonlinear response up to fracture. The transition from the linear to the nonlinear response is always attributed to the initiation of the matrix cracking [15]. The nonlinear responses of the stress versus strain result from the damage accumulation including matrix cracking and interfacial debonding or sliding [16]. The curves obtained at RT also present similar feature.

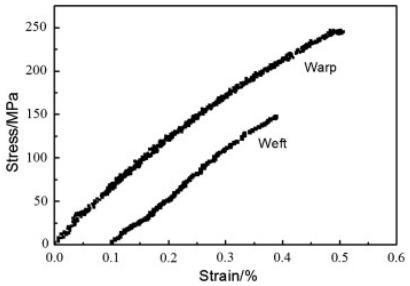

Fig. 3. Representative tensile stress–strain curves of the 2.5D-C/SiC composites in both warp and weft direction at 900 °C in air.

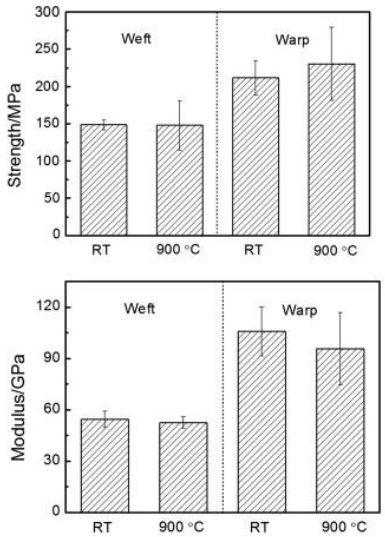

Fig. 4. Tensile properties of the 2.5D-C/SiC composite in weft and warp direction at RT and 900 °C in air. (a) Strength and (b) modulus.

Fig. 4 summarizes the UTS and modulus of the composite at RT and 900 °C in air. It is revealed that great anisotropy is present in the composite at warp and weft directions. The UTS and modulus in warp direction are about 1.5 times of those in weft direction. It is also indicated from Fig. 4 that the composite can retain its strength at 900 °C. The moduli at 900 °C are slightly lower than those at RT. The results suggest that there are negligible effects of the temperature (900 °C) on the tensile properties.

Fig. 5 shows the fatigue results of the 2.5D-C/SiC at RT and 900 °C. The figure is expressed as the applied maximum stress versus cycles to failure, i.e., *S–N* curves. Similar to the tensile properties, the fatigue limits also present significant anisotropy. The fatigue limits in warp direction are about 1.3–1.4 times of those in weft direction. Moreover, the composite display high resistance to the fatigue at RT. It can be found from Fig. 5a that the fatigue run-out was observed at a peak stress of 180 MPa (85% of the UTS) for 2.5D-C/SiC in warp direction. The fatigue limit in weft direction is about 84% of the UTS, shown in Fig. 5b. The fatigue limit at RT is much higher than the matrix cracking stress in either warp direction or the weft direction. It means that the composite can avoid the unsteady propagation of the matrix cracks, induced by the first loading during the fatigue, at fatigue limit [17].

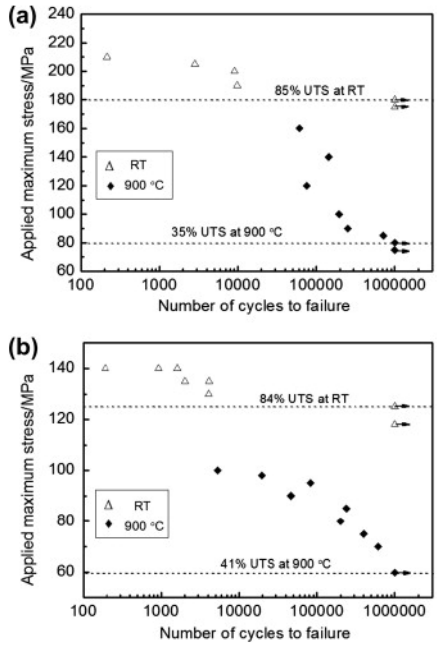

Fig. 5. *S–N* curves of the 2.5D-C/SiC at RT and 900 °C. (a) Warp direction and (b) weft direction.

Fig. 6 shows the stress–strain curves for fatigued specimens in weft direction at RT. For comparison, the tensile stress–strain curve of the virgin material is also included. The stress–strain behavior after the cyclic loading differed significantly from that for the virgin specimen. The UTS of is higher for the fatigued composites, however, the modulus decreases. Moreover, the linear parts in the curves were extended and fracture strain was larger for the fatigued specimen. Similar results can also be found on the stress–strain curves of the fatigued specimens in warp direction. The increase in strength is in agreement with those observed on other composites [18] ; [19].

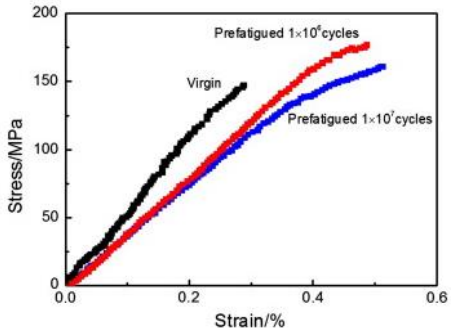

Fig. 6. Tensile stress–strain curves for the virgin and fatigued specimens at RT.

Fig. 7 displays the fractured surface of the specimen failed under cycle loading at RT. It can be found from Fig. 7a that the fracture mainly occurs in the warp fiber bundles for the composite cyclically loaded in the warp direction. The fractured plane of each bundle is not co-planar. The macroscopic presentation of the fractured surface is similar at various stress levels. Macroscopically, there were no different features for the fractured surface at 900 °C.Fig. 7b and c shows the fractured surface morphology for the composite in the weft direction at RT and 900 °C, respectively. The failure of the weft fiber bundles can be seen and the warp fiber bundles is almost intact at RT, however, both the weft and warp fiber bundles failed at 900 °C.

Previous researches put forward three fracture modes of the fiber bundles loaded in tension[13], shown in Fig. 8. The fracture of the 0° bundles in mode A originates from the crack propagation in 90° bundles. In mode B, the fracture occurs at the crossover points of 0°/90° bundles. The third mode (mode C) is caused by two cracks originating from two crossover points and indicative of interlaminar shear fracture within the fiber bundles. Therefore, the fracture caused by the cycle loading in warp direction are mainly composed of the second mode, and mixed with the third mode locally. For the

composites loaded in weft direction, the failure is composed of the mode B at RT and mode A at 900 °C.

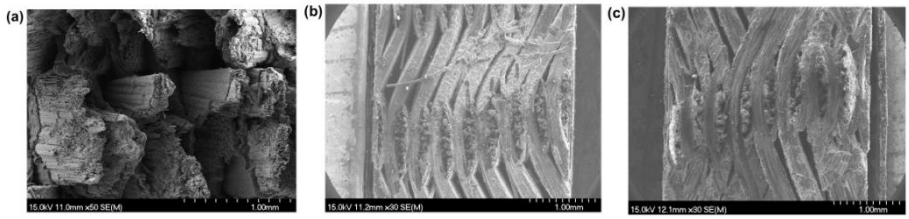

Fig. 7. SEM images of the fractured morphology for fatigued 2.5D-C/SiC. (a) Warp direction, RT, (b) weft direction, RT, and (c) weft direction, 900 °C.

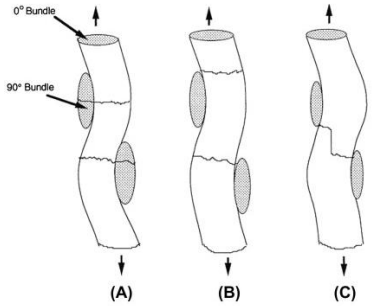

Fig. 8. Schematic illustration of three fracture modes for the fiber bundles [10].

Fig. 9 shows the magnified SEM images of the fractured surface of the 2.5D-C/SiC composite in warp direction at RT and 900 °C. It clearly shows that there was relatively more fiber pull-out for the specimen at 900 °C. Moreover, the length of the pull-out was larger. Similar results can also be found on the fractured surfaces fatigued in weft direction. The interfacial strength between fiber and matrix can be inferred from the length of the fiber pullout. The shear strength of the interface τi can be calculated by the equation: $\tau i = \sigma f d/2Lc$[20]. where σf is the fiber strength, d the diameter of the fiber, and Lc the shortest length of the broken fiber. Generally, the fiber pull-out length can be considered as $Lc/2$. Therefore, the longer pullout of the fiber indicates the smaller interface strength between the fiber and matrix at 900 °C, in agreement with the results obtained by Mizuno et al. [13].

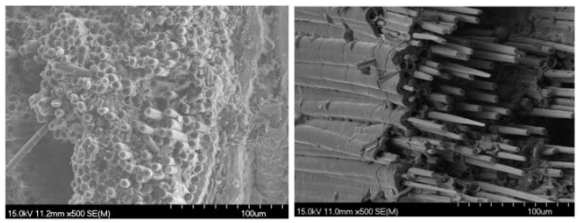

Fig. 9. Fractured surface of the fatigue composite failed in warp direction at RT and 900 °C. Extensive fiber pullout can be found on the specimen fractured at 900 °C.

Fig. 10 shows a cross-section image of a fatigued composite at 900 °C. It clearly displays that the broken matrix around the fibers. Meanwhile, upon the cyclic loading, weave stretching and aligning mechanisms could easily occur with the relief of strain mismatch, allowing longitudinal bundles to stretch. The process reduced the extent of the severity of localized stresses in the composite and allowed more uniform loading of the bundles. Therefore, a higher strain to failure and strength (Fig. 6), compared with the virgin composite, are achieved.

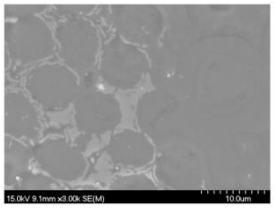

Fig. 10. Spallation of the SiC matrix in fatigued 2.5D-C/SiC, failed by the cyclic loading at 900 °C.

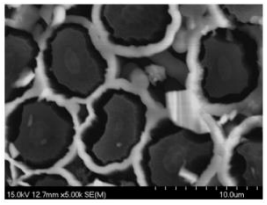

Fig. 11. SEM image of a 2.5D-C/SiC specimen fatigued at 900 °C. The carbon fibers were oxidized.

As mentioned above, many cracks could form within the composite during fatigue. The cracks offered the channels for the oxygen to diffuse into the composite. Therefore, the carbon fibers within the composite were heavily oxidized. Fig. 11 shows a typical example showing the oxidized carbon fibers within the SiC matrix. The consumption of the fiber could decrease the effective loaded area of the fibers and contributes to the degradation of the strength.

4. Conclution

The tension–tension fatigue properties were investigated for a 2.5D-C/SiC composite in warp and weft direction at RT and 900 °C in air. A series of fatigue tests were performed at different maximum stress levels in order to obtain the *S–N* curves. The damage mechanisms were revealed by observing the fractured morphology and measuring the residual tensile properties.

Acknowledgements

This work is supported by the National Natural Science Foundation of China(No. 11602066) and the National Science Foundation of Heilongjiang Province of China (QC2015058 and 42400621-1-15047), the Fundamental Research Funds for the Central Universities.

References

[1] P. Baiocco, S. Guedron, P. Plotard, J. Moulin The pre-X atmospheric re-entry experimental lifting body: program status and system synthesis Acta Astronaut, 61 (2007), pp. 459–474

[2] D. Filsinger, S. Münz, A. Schulz, S. Wittig Experimental assessment of fiber-reinforced ceramics for combustor walls J Eng Gas Turb Power, 123 (2001), pp. 271–276

[3] K.S. Lee, K.S. Jang, J.H. Park, T.W. Kim, I.S. Han, S.K. Woo Designing the fiber volume ratio in SiC fiber-reinforced SiC ceramic composites under hertzian stress Mater Des, 32 (2011), pp. 4394–4401

[4] Y. Katoh, L.L. Snead, C.H. Henager, A. Hasegawa, A. Kohyama, B. Riccardi, et al. Current status and critical issues for development of SiC composites for fusion applications J Nucl Mater, 367–370 (2007), pp. 659–671

[5] A.G. Evans, F.W. Zok, R.M. McMeeking Fatigue of ceramic matrix composites Acta Metall Mater, 43 (1995), pp. 859–875

[6] M.B. Ruggles-Wrenn, J. Delapasse, A.L. Chamberlain, J.E. Lane, T.S. Cook Fatigue behavior of a Hi–NicalonTM/SiC–B4C composite at 1200 °C in air and in steam Mater Sci Eng A, 534 (2012), pp. 119–128

[7] S. Momon, N. Godin, P. Reynaud, M. R'Mili, G. Fantozzi Unsupervised and supervised classification of AE data collected during fatigue test on CMC at high temperature Compos Part A – Appl Sci, 43 (2012), pp. 254–260

[8] S. Rudov-Clark, A.P. Mouritz Tensile fatigue properties of a 3D orthogonal woven composite Compos Part A – Appl Sci, 39 (2008), pp. 1018–1024

[9] J. Kim, P.K. Liaw Characterization of fatigue damage modes in nicalon/calcium aluminosilicate composites J Eng Mater Trans ASME, 127 (2005), pp. 8–15

[10] J. Andersons, M. Hojo, S. Ochiai Model of delamination propagation in brittle-matrix composites under cyclic loading J Reinf Plast Comp, 20 (2001), pp. 431–450

[11] S. Mall, K.J. LaRochelle Fatigue and stress-rupture behaviors of SiC/SiC composite under humid environment at elevated temperature Compos Sci Technol, 66 (2006), pp. 2925–2934

[12] Zh Su, Y. Kaneko, Y. Ochi, T. Ogasawara, T. Ishikawa Low cycle fatigue behavior in an orthogonal three-dimensional woven Tyranno fiber reinforced Si–Ti–C–O matrix composite Inter J Fatigue, 26 (2004), pp. 1069–1074
[13] M. Mizuno, S. Zhu, Y. Nagano, Y. Sakaida, Y. Kagawa, M. Watanabe Cyclic fatigue of SiC/SiC composites at room and high temperature J Am Ceram Soc, 79 (1996), pp. 3065–3077
[14] J.Q. Ma, Y.D. Xu, L.T. Zhang, L.F. Cheng, J.J. Nie, N. Dong Microstructure characterization and tensile behavior of 2.5D C/SiC composites fabricated by chemical vapor infiltration Scripta Mater, 54 (2006), pp. 1967–1971
[15] J.L. Kuhn, S.I. Haan, P.G. Charalambides Stress induced matrix microcracking in brittle matrix plain weave fabric composites under uniaxial tension J Compos Mater, 34 (2000), pp. 1640–1664
[16] M. Wang, C. Laird Characterization of microstructure and tensile behavior of a cross-woven C–SiC composite Acta Mater, 44 (1996), pp. 1371–1387
[17] M.B. Ruggles-Wrenna, D.T. Christensen, A.L. Chamberlain, J.E. Lane, T.S. Cook Effect of frequency and environment on fatigue behavior of a CVI SiC/SiC ceramic matrix composite at 1200 °C Compos Sci Technol, 71 (2011), pp. 190–196
[18] S.F. Shuler, J.W. Holmes, X. Wu Influence of loading frequency on the room-temperature fatigue of a carbon-fiber/SiC-matrix composite J Am Ceram Soc, 76 (1993), pp. 2327–2336
[19] N. Chawla, Y.K. Tur, J.W. Holms, J.R. Barber High-frequency fatigue behavior of woven-fiber-fabric-reinforced polymer-derived ceramic–matrix composites J Am Ceram Soc, 81 (1998), pp. 1221–1230
[20] D.B. Marshall, W.C. Oliver Measurement of interfacial mechanical properties in fiber-reinforced ceramic composites J Am Ceram Soc, 70 (1987), pp. 542–548